Talanta 111 (2013) 163–169

Contents lists available at SciVerse ScienceDirect

Talanta

journal homepage: www.elsevier.com/locate/talanta

One-step fabrication of integrated disposable biosensor based on ADH/NAD^+/meldola's blue/graphitized mesoporous carbons/chitosan nanobiocomposite for ethanol detection

Erhui Hua [a], Li Wang [a], Xiaoying Jing [a], Changtao Chen [b], Guoming Xie [a,*]

[a] Key Laboratory of Laboratory Medical Diagnostics of Ministry of Education, Department of Laboratory Medicine, Chongqing Medical University, No. 1 Yi Xue Yuan Road, Chongqing 400016, PR China

[b] Department of Automation Engineering, Sichuan College of Chemical Technology, Luzhou 646005, PR China

ARTICLE INFO

Article history:
Received 28 November 2012
Received in revised form
25 February 2013
Accepted 27 February 2013
Available online 7 March 2013

Keywords:
One-step
Graphitized mesoporous carbons
Meldola's blue
Electrochemical biosensor
NADH
Ethanol

ABSTRACT

A novel strategy to simplify the dehydrogenase-based electrochemical biosensor fabrication through one-step drop-coating nanobiocomposite on a screen printed electrode (SPE) was developed. The nanobiocomposite was prepared by successively adding graphitized mesoporous carbons (GMCs), meldola's blue (MDB), alcohol dehydrogenase (ADH) and cofactor nicotinamide adenine dinucleotide (NAD^+) in chitosan (CS) solution. MDB/GMCs/CS film was prepared. Cyclic voltammetry measurements demonstrated that MDB was strongly adsorbed on GMCs. After optimizing the concentration of MDB and the working potential, the MDB/GMCs/CS film presented a fast amperometric response (5 s), excellent sensitivity (10.36 nA μM^{-1}), wide linear range (10–410 μM) toward NADH and without any other interference signals (such as AA, UA, DA, H_2O_2 and metal ions). Furthermore, concentrations of ADH and NAD^+ in nanobiocomposite and the detection conditions (temperature and pH) were also optimized. The constructed disposable ethanol biosensor showed an excellent linear response ranged from 0.5 to 15 mM with high sensitivity (67.28 nA mM^{-1}) and a low limit of detection (80 μM) and a remarkable long-term stability (40 days). The intra-batch and inter-batch variation coefficients were both less than 5% ($n=5$). The ethanol recovery test demonstrated that the proposed biosensor offered a remarkable and accurate method for ethanol detection in the real blood samples.

1. Introduction

The accurate determination of ethanol in complex specimens is very important in clinical and forensic medical [1]. Additionally, this is also a significant determinant in controlling the fermentation process and product quality in the beverage, food and other industries [2]. In the past several decades, numerous methodologies have been developed for such an analysis, including refractometry [3], liquid chromatography [4], gas chromatography [5] and spectrophotometer [6]. Recently, an electrochemiluminescence ethanol biosensor was also developed [7]. In spite of these the methodologies could accurately quantify the ethanol from complex samples, however, the characteristics, such as the time consuming process, complex to perform, laborious sample pre-treatment and expensive instrumentations [8], have, for the moment, become more difficult to meet the need of fast and *in-situ* measurements. The electrochemical biosensor has drawn tremendous attention with excellent properties, including a good sensitivity, easy adaptability for *in-situ* analysis, relatively inexpensive instrument [9] and less reagent consumption.

Actually, a great number of electrochemical biosensors based on alcohol oxidase (AOX) and alcohol dehydrogenase (ADH) for ethanol detection, have been reported in the past several decades [10–15]. ADH-based biosensor is superior to AOX-based compared with the natures of stability and specificity [16]. ADH catalyzes the conversion of ethanol to acetaldehyde in alkaline condition in the presence of cofactor NAD^+ (an oxidized form of nicotinamide adenine dinucleotide) and a reduced form of NADH generated, which would be detected on the electrode system. Considering constructing a reagent-less biosensor for rapid and accurate determination of ethanol in the complex samples, several major problems should be overcome: (1) the large overpotential of NADH on the traditional bare electrodes leads to the electrode surface fouling and ultimately results in an electrode system lacking sensitivity and stability [17]; (2) at the large overpotential, the electroactive molecules coexisting with NADH, such as ascorbic acid (AA), uric acid (UA) and dopamine (DA), are also readily oxidized, causing a very poor specificity of the

* Corresponding author. Tel./fax: +86 23 68485239.
E-mail address: guomingxie@cqmu.edu.cn (G. Xie).

0039-9140/$ - see front matter © 2013 Elsevier B.V. All rights reserved.
http://dx.doi.org/10.1016/j.talanta.2013.02.064

biosensor [18]; (3) the leakage of NAD^+ modified on the columnar electrode renders the biosensor unstable when the measurement was performed. Considerable efforts have been devoted to synthesizing novel nanomaterials to decrease the electrooxidation overpotential as well as to increase the sensitivity of the biosensor toward NADH in the past several decades [19,20]. Nonetheless, the potential is not decreased enough and the interference of AA is still existing [21,22]. Additionally, cofactor NAD^+ is used as a reagent mixed with samples [13,23,24]. Recently, several novel strategies and materials are also developed to overcome these problems in constructing a reagent-less dehydrogenase-based biosensor [9,25–27]. ADH and NAD^+ were immobilized on the Nafion/MWCNTs/Au NPs/Meldola's blue (MDB) composite film in our previous research and the high stability of the proposed biosensor was obtained [1]. These above studies present an outstanding performance for the real sample analysis. However, the fabrication of dehydrogenase-based biosensor often includes several step-by-step procedures for surface immobilization of enzyme and NAD^+ and electrocatalysts, which were technically complicated and time-consuming [28,29]. Multiple steps for biosensor fabrication inevitably make it difficult to minimize the biosensor-to-biosensor deviation [9]. Consequently, more efforts should be made to simplify the fabrication procedures of dehydrogenase-based biosensor.

The past few years have seen an explosion in the use of ordered mesoporous carbons (OMCs) to design novel biosensors [30–32]. This kind of material offers attractive features that can be exploited in electrochemistry, such as good electronic conductivity, high specific surface area, large pore volume and size, and wide open ordered structure [31]. Several studies have pointed out that OMCs can be used for adsorption of dyes [33,34], implying that the OMCs have great potential in developing mediator-based biosensor. Graphitized mesoporous carbons (GMCs), possessing the features of structural homogeneity with significant graphite-like domains and stacking heights, have also been identified as a promising material for use in high-performance components in electrochemical applications [35].

In this study, a novel strategy was developed to immobilize MDB on the electrode through GMCs adsorption. Electrochemical characters of MDB/GMCs/CS film toward NADH were investigated. Furthermore, the nanobiocomposite, including ADH, NAD^+, MDB, GMCs, and CS, was prepared for one-step fabrication of reagent-less dehydrogenase-based biosensor. In this system, CS, with its cationic nature, remarkable film-forming property and excellent biocompatibility, not only acted as a dispersing agent for GMCs, but also as a binding factor for ADH immobilization. Screen printed electrode (SPE) has been widely used in electrochemical biosensing due to the inherent superiority of its manufacturing process, which is inexpensive, rapid and capable of mass production [36]. Three-electrode system SPE was employed to develop disposable dehydrogenase-based biosensor. The performances of the integrated biosensor toward ethanol were investigated. Additionally, stability of MDB in different conditions was also evaluated. Compared to the existing methods for fabrication of dehydrogenase-based biosensor, the strategy demonstrated here was facile and efficient. The ability of the biosensor for real sample analysis was also evaluated.

2. Experimental

2.1. Reagents

ADH (EC. 1.1.1.1, 390 U mg^{-1} protein, from *Saccharomyces cerevisiae*) and Meldola's blue were purchased from Sigma. β-nicotinamide adenine dinucleotide trihydrate (oxidized form, NAD^+, >97%), β-nicotinamide adenine dinucleotide reduced dipotassium salt (reduced form, NADH, 92%), L-ascorbic acid (AA, >99%), uric acid (UA, >99%), dopamine hydrochloride (DA, >99%), Tris and chitosan (CS, deacetyiation, 90–95%) were obtained from BBI. Graphitized mesoporous carbons (GMCs, particle size <500 nm) were obtained from Aldrich without further purification. All other reagents were of analytical grade and used as received. Water (resistivity, 18.2 MΩ) was purified using the Millipore-Q water purification system. The fresh and normal whole blood samples (EDTA-2K anticoagulation) utilized in this study were collected from the First Affiliated Hospital of Chongqing Medical University.

2.2. Apparatus and instrumentations

Amperometric and cyclic voltammetric measurements were performed on an electrochemical workstation (CHI660D, Chenhua Instrument Company of Shanghai, China). A disposable screen printed electrode (SPE, diameter, 3 mm; geometric area, 0.071 cm^2) consisting of a carbon working electrode, a carbon counter electrode and a silver pseudo-reference electrode was purchased from Deltabiotech (B1008153, China) and used as received. UV–vis absorbance spectroscopy was performed using a NanoDrop spectrophotometer (ND-1000, Thermo Fisher Scientific, USA). All experiments were performed at room temperature (25 ± 2 °C) unless otherwise stated.

2.3. Preparation of NADH biosensors

2 mg GMCs were firstly dispersed in 1 ml CS (0.5% solution in 0.05 M HCl, the pH was adjusted to 6.0 using 1.0 M Tris aqueous solution) by ultrasonic for 15 min, then 10 μl 10 mM MDB aqueous solution was added and allowed to mix overnight at 4 °C. In control experiments, GMCs/CS and MDB/CS suspension were also prepared. 5 μl MDB/GMCs/CS, GMCs/CS and MDB/CS suspension were uniformly coated on the working electrode of the SPE and allowed to dry at 4 °C (approximately 6 h). In order to optimize the concentration of MDB, various volumes of MDB (1 μl, 4 μl, 7 μl, 10 μl and 13 μl) were added in the GMCs/CS suspension.

2.4. Preparation of nanobiocomposite and construction of ethanol biosensor

The following optimized procedures were used for the preparation of nanobiocomposite. MDB/GMCs/CS suspension was reprepared with the previous procedures just doubling the concentration of GMCs, MDB and CS. 100 μl ADH (16 mg ml^{-1} in Tris–HCl solution, 0.1 M, pH 6.0) and 100 μl NAD^+ (16 mM in Tris–HCl solution, 0.1 M, pH 6.0) were successively mixed with 200 μl reprepared MDB/GMCs/CS suspension by gently shaking. After that, 5 μl nanobiocomposite was carefully coated on the naked SPE and allowed to dry at 4 °C in darkness (approximately 6 h).

2.5. Preparation of integrated biosensor for real sample analysis

In order to adjust the pH value of samples to 8.0 when measurements performed, a 10 μl drop of the Tris–HCl (0.1 M, pH 8.0) was placed onto the SPE near to (but not on) the working electrode and allowed to dry at room temperature. After nanobiocomposite was coated and dried, a hydrophilic membrane with a hole was placed over the ethanol biosensor with double-sided adhesive tape to control the volume of samples on the SPE [1] (shown in Scheme 1).

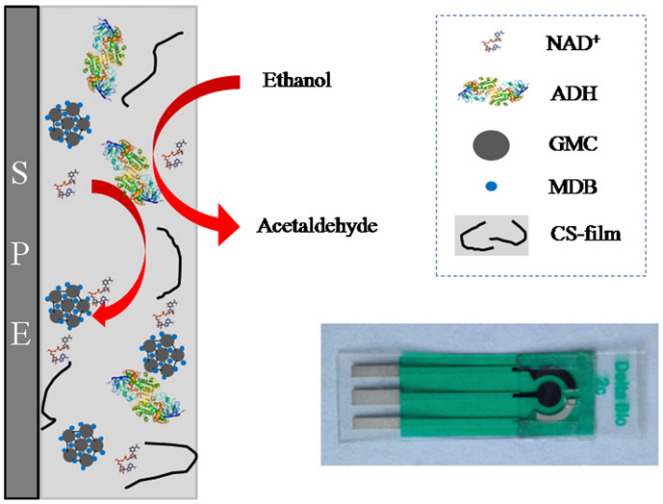

Scheme 1. Schematic illustration of the integrated ethanol biosensor constructed with nanobiocomposite and a photograph of the SPE with hydrophilic membrane.

2.6. Electrochemical detection of NADH and ethanol

Cyclic voltammetry and amperometric trace of MDB/GMCs/CS/SPE towards NADH were recorded in Tris–HCl solution. The amperometric measurements of ethanol in Tris–HCl buffer solution (0.1 M, pH 8.0) were performed. As for a real blood sample detection, 20 s were used for sample filling in the electrode and adjusting the pH of the sample to 8.0, and 5 s for amperometric measurement. The volume of a sample dropped on the SPE was 10 μl. All the experiments had been repeated at least three times and reproducible results were obtained.

2.7. Absorbance of MDB

0.05 mM MDB in CS (0.5% solution in 0.05 M HCl, pH was adjusted to 6.0 with 1.0 M Tris) and 0.04 mM MDB in Tris–HCl solution (0.1 M, pH 8.0) were prepared. UV–vis absorption spectrum of MDB were measured and the absorbances were recorded at 560 nm. When not in use, these solutions were stored at 4 °C in darkness.

3. Results and discussion

3.1. Electrochemical behaviors of MDB/GMCs/CS/SPE

Cyclic voltammetry was used to investigate the electrochemical behaviors of MDB adsorbed in GMCs/CS composite film. The MDB/GMCs/CS/SPE exhibited a pair of distinct redox peak in Tris–HCl buffer solution (Fig. 1A) and a plot of oxidation and reduction peak currents as a function of scan rates were linear up to 0.1 V s^{-1} (the inset of Fig. 1A), suggesting facile surface-confined charge transfer kinetics. In addition, redox peak currents of MDB were almost without visible changes after 20 successive scans (data not shown). In control experiments, MDB/CS composite modified SPE was also prepared. After washing with ultrapure water, the MDB/CS/SPE only showed a tiny and unstable redox peak in Tris–HCl buffer solution (Fig. 1B, dash dot line). All these results clearly implied that MDB was strongly adsorbed on the GMCs. The reason may be explained by that the mesoporous carbons with open pore structure, large pore size and carbonaceous surfaces could be advantageous in bulky molecular and dyes adsorption [33,34].

The concentration of MDB in GMCs/CS composite was optimized. With the increasing concentration of MDB from 0.01 to 0.1 mM, the oxidation peak current obviously increased (data not shown). However, the current did not obviously increase and the leakage of MDB on the SPE appeared when the concentration reached to 0.13 mM (the color of the buffer solution on the SPE changed from lucency to lilac), indicating that the adsorption sites of GMCs for MDB was almost saturated. Consequently, 0.1 mM MDB was optimized for preparing MDB/GMCs/CS composite.

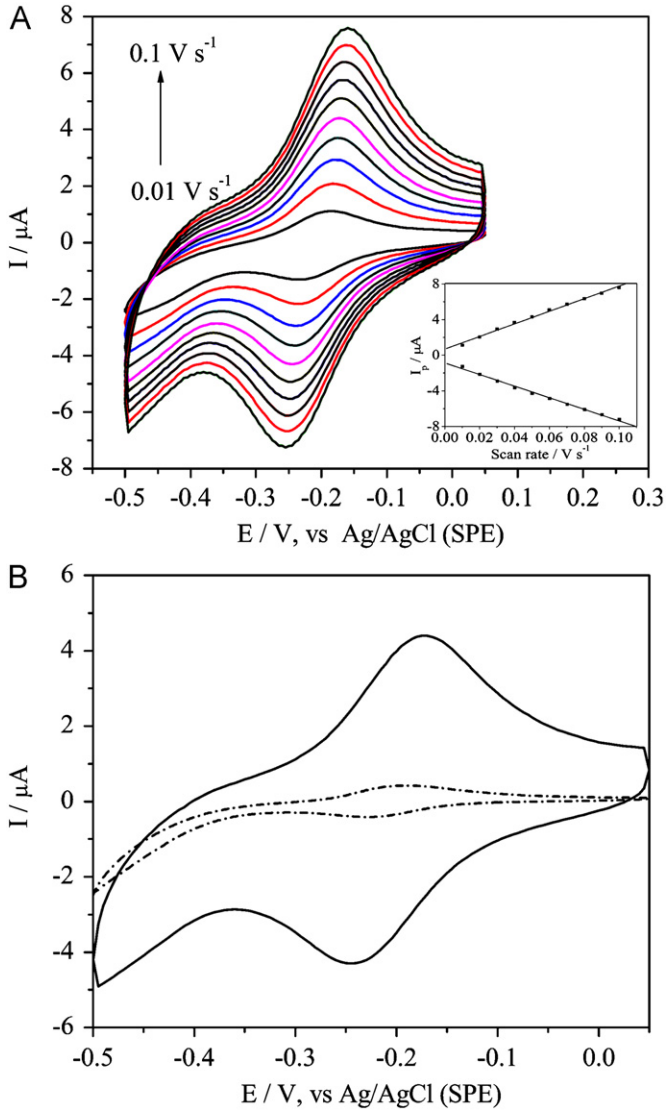

Fig. 1. (A) Cyclic voltammograms of the MDB/GMCs/CS/SPE with different scan rates: 0.01, 0.02, 0.03, 0.04, 0.05, 0.06, 0.07, 0.08, 0.09 and 0.1 V s^{-1} in Tris–HCl buffer solution (0.1 M, pH 8.0). The inset shows the relationship of oxidation peak and reduction peak currents versus scan rates and (B) cyclic voltammograms of the MDB/GMCs/CS/SPE (solid line) and MDB/CS/SPE (dash dot line) in Tris–HCl buffer solution (0.1 M, pH 8.0). Scan rate: 0.05 V s^{-1}.

3.2. Electrocatalytic activities of the MDB/GMCs/CS/SPE toward NADH

Cyclic voltammetry studies were conducted with the MDB/GMCs/CS/SPE and GMCs/CS/SPE in the absence and presence of NADH (shown in Fig. 2). The typical redox peak of MDB in MDB/GMCs/CS/SPE was obtained as stated earlier. When the NADH was presented, the oxidation peak current was obviously increased and the whole process could be illustrated as follows [37]:

$$NADH + MDB^{+} \rightarrow NAD^{+} + H^{+} + MDBH \quad (1)$$

$$MDBH \rightarrow M\,DB^{+} + H^{+} + 2e^{-} \quad (2)$$

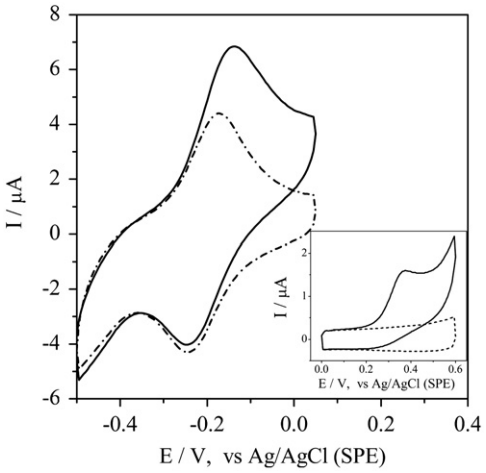

Fig. 2. Cyclic voltammograms of the MDB/GMCs/CS/SPE and GMCs/CS/SPE (inset) in Tris–HCl buffer solution (0.1 M, pH 8.0) with the absence (dash dot line) and presence (solid line) of 0.2 mM NADH. Scan rate: 0.05 V s^{-1}.

With the aid of MDB, the oxidation peak potential of NADH on the MDB/GMCs/CS/SPE occurred at −0.14 V, which was significantly lower than GMCs/CS modified SPE (0.37 V) and bare SPE (0.8 V, data not shown). Moreover, the current increase was larger than GMCs/CS. The lower oxidation potential and higher oxidation current suggested that the MDB adsorbed onto GMCs acted as a very efficient electrochemical mediator for NADH oxidation.

3.3. Selectivity of the MDB/GMCs/CS/SPE toward NADH

It was feasible to introduce a relatively lower potential as well as provide the highly efficient catalytic properties of the MDB/GMCs/CS/SPE toward NADH. Interference-free is also a very important property of the constructed biosensor. The main interferences are due to other electroactive molecules, such as AA, UA and DA. Some mediator modified electrodes, which presented the perfect electrocatalytic activity toward NADH, failed to overcome the interference due to AA, as these mediators could also catalyze the oxidation of AA [38]. Despite the fact that anionic polymers like Nafion or Kodak AQ [39], could prevent the approach of AA to the electrode, however, these polymers could also seal off the active site of nanomaterials to electrooxidation of NADH. In the present investigation, the analytical performance of the MDB/GMCs/CS/SPE toward NADH was monitored at two typical operation potentials (−0.1 V and −0.15 V) in the presence of several potential interferences (shown in Fig. 3). In all cases, UA, H_2O_2, DA, and other metal ions, did not show obvious interferences to NADH. Nevertheless, AA emerged serious oxidation current response at −0.1 V. When the potential changed to a more negative (−0.15 V), the interference was completely eliminated while the response of NADH still maintained high sensitivity, implying that MDB was an appropriate mediator for interference-free detection of NADH. Consequently, the working potential was chosen at −0.15 V in the next experiments.

3.4. Dynamic range of the MDB/GMCs/CS/SPE toward NADH

The potential utility of the MDB/GMCs/CS/SPE was further examined by recording the amperometric response of different concentrations of NADH. Fig. 4A displays the amperometric traces versus the concentrations of NADH on the GMCs/MDB/CS/SPE at −0.15 V. The fast and stable responses were obtained within 5 s upon every injection. The current responses were linear with the concentrations of NADH ranged from 10 μM to 410 μM (shown in

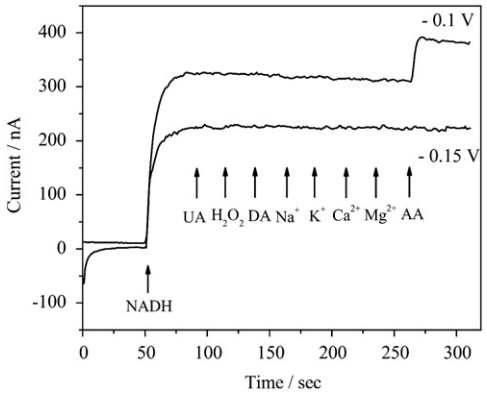

Fig. 3. Amperometric responses of the MDB/GMCs/CS/SPE upon successive addition of 15 μM NADH, 500 μM UA, 100 μM H_2O_2, 500 μM DA, 100 μM NaCl, 100 μM KCl, 100 μM $CaCl_2$, 100 μM $MgCl_2$ and 500 μM AA with operational potentials of −0.1 V and −0.15 V in a stirred Tris–HCl buffer solution (0.1 M, pH 8.0, 300 rpm).

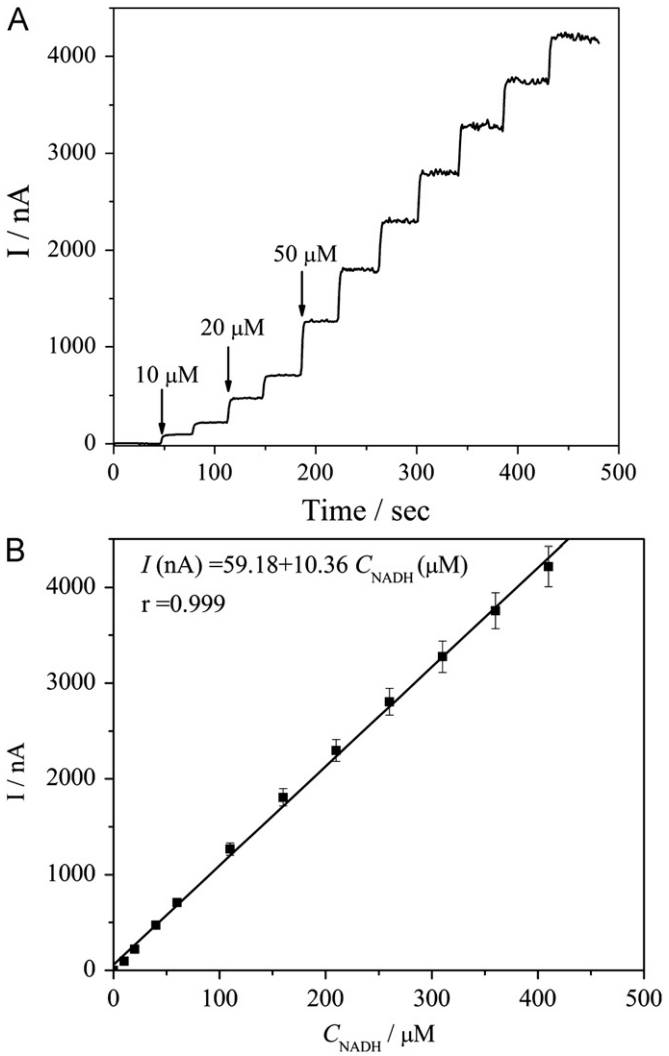

Fig. 4. (A) Amperometric responses of the MDB/GMCs/CS/SPE upon successive addition of NADH (10, 20 and 50 μM) in a stirred Tris–HCl buffer solution (0.1 M, pH 8.0, 300 rpm) and (B) the corresponding calibration curve of the response currents and the concentrations of NADH. Working potential: −0.15 V. The error bars indicate 95% confidence interval of steady-state currents.

Fig. 4B). A linear regression equation of I (nA)=59.18+10.36C (μM) was established with a correlation coefficient of 0.999. The limit of detection (LOD) was also estimated to be around

0.186 μM based on a signal-to-noise ratio of 3 ($S/N=3$). The excellent analytical characteristics of the GMCs/MDB/CS/SPE were attributed to the fact that the good dispersion of GMCs in the CS film and highly intimate contact with MDB, provided a three-dimensional electron conductive network, accordingly facilitated the charge transport [40].

3.5. Electrocatalytic characters of ADH/NAD^+/MDB/GMCs/CS/SPE toward ethanol

Since the MDB/GMCs/CS/SPE exhibited a high sensitivity and excellent selectivity toward NADH, it could be used for the development of dehydrogenase-based biosensor. The ethanol biosensor was constructed using the prepared nanobiocomposite including ADH, NAD^+, MDB, GMCs and CS described earlier. The principle is shown in Scheme 1. With the objective of simplifying the detection procedure and decreasing the waste of NAD^+ when the measurement was carried out, cofactor NAD^+ was modified on the surface of the electrode together with ADH. It is important to remark that although the cofactor could not be immobilized on the electrode and readily to leak into the solution when the measurement was carried out, the volume of the sample could be controlled around 10 μl via hydrophilic film. Therefore, influence of the cofactor leakage was negligible in this experiment.

Because the ethanol biosensor response depended on the amount of the immobilized ADH and NAD^+, various ADH ($1\sim9$ mg ml^{-1}) and NAD^+ (1–6 mM) loadings were analyzed, respectively (shown in Fig. 5A and B). The current responses of ethanol biosensors increased with the concentrations of ADH from 1 to 4 mg ml^{-1} and NAD^+ from 1 to 4 mM. However, reduced responses were obtained with more ADH loading. The same responses were also obtained when concentrations of NAD^+ increased more than 4 mM. Consequently, 4 mg ml^{-1} ADH and 4 mM NAD^+ were chosen as the optimal concentrations of enzyme and cofactor, respectively. The effects of temperature and pH to the ethanol biosensor were also investigated (shown in Fig. 4C and D). The highest amperometric responses were observed at 35 °C and pH 8.0, respectively. It should be noted that the ethanol biosensor displayed almost no response in neutral and weak acid environments, because the redox reaction of ADH catalyzing ethanol is reversible. ADH catalyzes the conversion of ethanol to acetaldehyde in alkaline environment; however, the reaction would reverse in neutral condition.

Under the optimized condition, the performances of the integrated biosensor were evaluated by amperometric response experiments. Fig. 6 presents the steady-state response of the proposed biosensor for different concentrations of ethanol in Tris–HCl buffer solution. The currents increased linearly with the ethanol concentrations over the range from 0.5 to 15 mM with the high sensitivity of 67.28 nA mM^{-1} (the inset of Fig. 6). The limit of detection (LOD) and the limit of quantitative determination (LQ) were estimated to be 80 μM ($S/N=3$) and 267 μM ($S/N=10$), respectively. The LOD of the proposed biosensor for ethanol detection was lower than those achieved with the Nafion/ADH/NAD^+/TBO/GCE [2] and AOX/polvinylferrocenium/Pt electrode [41]. The electrode-to-electrode reproducibility was also evaluated. Five integrated biosensors prepared with the same procedure were tested, and the relative standard deviation (RSD) was found to be 3.8% for 4 mM ethanol and 4.6% for 10 mM ethanol. The excellent reproducibility strongly confirmed that the use of rationally designed nanobiocomposite for one-step fabricating biosensor remarkably minimized the biosensor-to-biosensor deviation. Stability of the fabricated biosensor was also examined. After 40 days, the amperometric responses of the biosensors

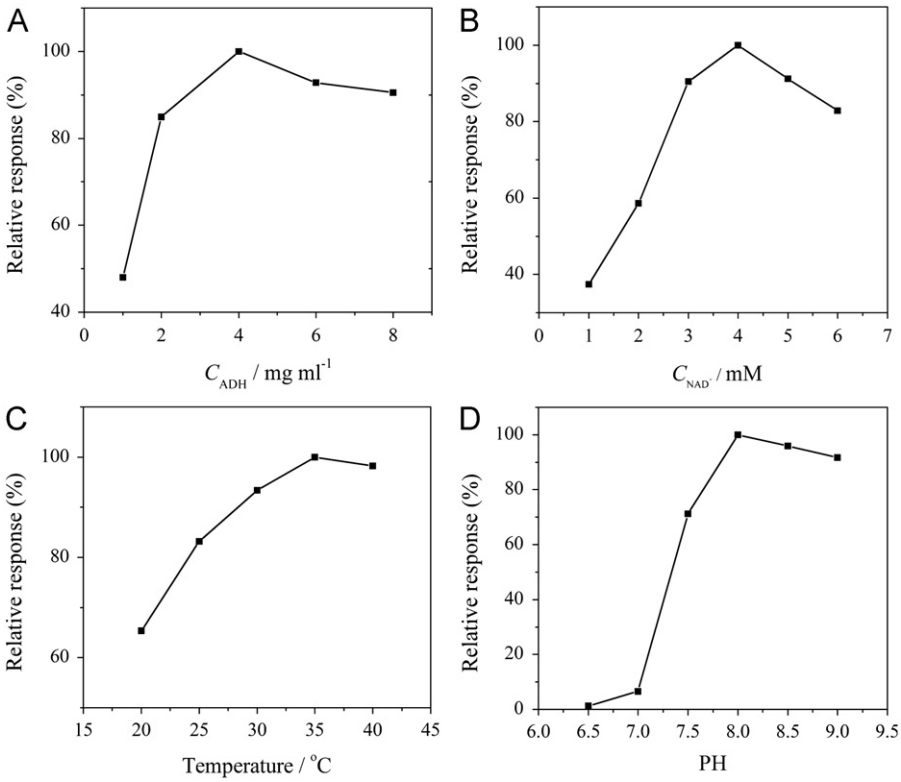

Fig. 5. Optimization of the concentrations of ADH and NAD^+ loading and detect conditions. (A) Effects of ADH concentrations on the amperometric responses of ethanol biosensors, NAD^+ loading, 3 mM; ethanol in Tris–HCl (0.1 M, pH 8.0), 5 mM, (B) effects of NAD^+ concentrations on the amperometric responses of ethanol biosensors, ADH loading, 5 mg ml^{-1}; ethanol in Tris–HCl (0.1 M, pH 8.0), 5 mM, (C) effects of temperature and (D) pH on the amperometric responses of ethanol biosensors, ADH loading, 4 mg ml^{-1}; NAD^+ loading, 4 mM; ethanol, 5 mM. Applied potential: −0.15 V.

toward 4 mM ethanol remained 91 ± 2.4% (n=5) compared with the freshly prepared biosensors. The high stability could be attributed to the good biocompatibility of GMCs and CS for the enzyme and cofactor NAD^+ and appropriate weak acid microenvironment for MDB. Compared the results with the literature data (given in Table 1), the biosensor proposed here was acceptable and satisfactory.

3.6. Determination of ethanol in real samples

The point-of-care device requires rapid determination and no sample preparation. In order to achieve that ethanol detection was directly performed without any pre-treatment, in our previous study, the pH of the working electrode was adjusted to around 8.0 via coating Tris–HCl solution (0.1 M, pH 8.0) upon the nanobiocomposite film. However, the response of the biosensor to ethanol obviously decreased after it was stored for 7 days at 4 °C in darkness, whereas, the same situation did not present when the nanobiocomposite film was coated with nothing. The same phenomenon was also presented on the NADH biosensor. With a suspicion, the stability of MDB in CS/Tris–HCl solution (pH 6.0) and Tris–HCl solution (pH 8.0) was evaluated by UV–vis absorbance spectroscopy (shown in Fig. 7). A sharply decreased relative absorbance of MDB was observed in Tris–HCl solution (pH 8.0) after 10 days. While, the high relative absorbance of MDB still remained in CS/Tris–HCl solution even after 30 days. This condition strongly indicated that MDB was greatly stable in CS/Tris–HCl solution than in an alkaline environment. The decreased absorbance likely attributed to the degradation of MDB. This phenomenon could explain the decrease response of the ethanol biosensor. For this reason, the Tris–HCl solution (0.1 M, pH 8.0) was added nearby the electrode for constructing integrated biosensor.

With the purpose of evaluating the feasibility, the proposed biosensor was employed for the determination of ethanol in real samples. No ethanol was detected in normal samples. While the blood ethanol concentration of the drinkers is often high and could be detected with the proposed biosensors without prediluted for its wide linear range. Therefore, the standard ethanol concentrations (1.00, 5.00 and 10.00 mM) were adopted to evaluate the possibility of the ethanol detection in blood samples. Table 2 summarizes the background and the recoveries of ethanol in blood samples obtained by the proposed biosensors. As can be observed, the recovery percentages ranged from 97.2% to 106.0%, indicating good accuracy for ethanol detection.

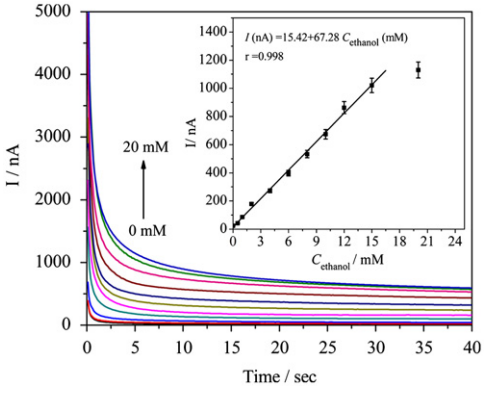

Fig. 6. Amperometric responses recorded with the ADH/NAD^+/MDB/GMCs/CS/SPE for different concentrations of ethanol ranged from 0 to 20 mM. Inset: the calibration curve of response currents and the concentration of ethanol. The response currents were read out at 5 s and the data were average values from five modified electrodes. The error bars indicate the standard deviation of five determinations.

4. Conclusion

In summary, a novel strategy has been demonstrated to simplify the fabrication of ADH-based electrochemical biosensor through rationally designed nanobiocomposite and one-step fabrication of the integrated biosensor. The mediator MDB was strongly adsorbed

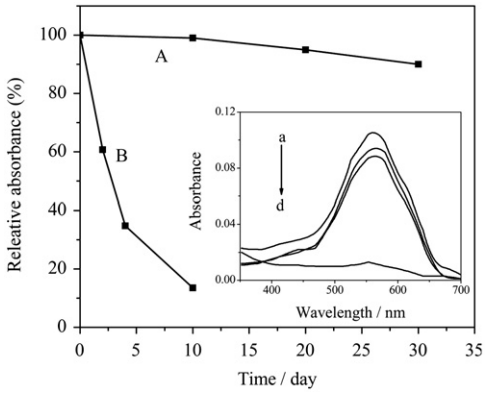

Fig. 7. Relative absorbance of MDB in (A) CS/Tris–HCl solution (pH 6.0) for 30 days and (B) Tris–HCl solution (pH 8.0) for 10 days. Inset presents the absorption spectrum of MDB in CS/Tris–HCl solution (a) before and (b) after 30 days, and in Tris–HCl solution (c) before and (d) after 10 days.

Table 1
Analytical characteristics of ADH-based biosensors for ethanol detection.

Biosensors[a]	Linear range (mM)	Sensitivity (nA/mM)	LODs[b] (μM)	Storage stability	Ref.
Nafion/ADH/TBO/GCE	2480–6610	0.12	n.g. [c]	Stable for 84 h	[2]
Nafion/ADH/NAD^+/TBO/GCE	283–856	1.4	29000	n.g.	[2]
Nafion/ADH/Graphene/GCE	0.2–21	n.g.	0.025	89% of initial response after two weeks	[42]
ZrO_2/PAF/GCE	0.03–1	33.87	n.g.	n.g.	[43]
	1–10	6.70			
Au/SiO_2/GCE	0.01–1	26.39	n.g.	n.g.	[44]
	1–10	5.38			
ADH/IL/Graphene/CS/GCE	0.025–0.2	483.7	5	82.8% of initial response after 15 days	[45]
ADH/MDB/OMC/GCE	Up to 6	34.58	19	22.3% of initial sensitivity after half a month	[37]
ADH/PBCB/SWNT/GCE	0.4–2.4	n.g.	90	80% of original response after 30 days	[46]
Nafion/ADH/PDDA/SWNTs/GCE	0.5–5	n.g.	90	~74% of original response after 25 days	[47]
ADH/PVA/MWCNT/GCE	Up to 1.5	196	13	~50% of initial current after 7 days	[48]
ADH/NAD^+/MDB/GMCs/SPE	0.5–15	67.28	80	91% of freshly prepared biosensors after 40 days	This work

[a] TBO, toluidine blue O; PAF, poly(acid fuchsin); IL, 1-(3-aminopropyl)-3-methylimidazolium bromide; OMC, ordered mesoporous carbon; PBCB, poly(brilliant cresyl blue); PDDA, poly(dimethyldiallylammonium chloride); PVA, poly(vinyl acetate); MWCNT, multiwalled carbon nanotube.
[b] LOD, limit of detection.
[c] n.g., data not given.

Table 2
Recovery percentages of ethanol in different whole blood samples obtained with the integrated biosensors.

Sample	Background[a] (mM)	$C_{ethanol}$ added (mM)	$C_{ethanol}$ found[b] (mM)	Recovery (%)
1	0	1.00	1.06	106.0
2	0	5.00	4.86	97.2
3	0	10.00	10.53	105.3

[a] When the current responses of integrated biosensors for ethanol were less than 20 nA, the background values were recorded 0 mM.
[b] Average of three measurements.

on the GMCs and furthermore, remarkably increased the response of electrocatalytic oxidation of NADH. Under the optimized conditions, the integrated ADH-based biosensor exhibited excellent performance for ethanol detection, such as a large linear range, a low detection limit, outstanding long-term stability and small biosensor-to-biosensor deviation. Moreover, the proposed ethanol biosensor was successfully used for the real blood sample analysis without any pre-treatment. The strategy demonstrated here likely to be versatile for simplifying the fabrication of other disposable dehydrogenase-based biosensor for the practical and on-site measurement.

Acknowledgments

We are grateful for the financial supports from the Foundation of National Key Discipline in Laboratory Medicine, Chongqing Medical University (No. 201202) and Luzhou City Science and Technology Planning Project (No. 2012-s-42 (2/5)).

References

[1] S.H. Zhen, Y. Wang, C.G. Liu, G.M. Xie, C.S. Zou, J. Zheng, Y. Zhu, Forensic Sci. Int. 207 (2011) 177–182.
[2] A.P. Periasamy, Y. Umasankar, S.M. Chen, Talanta 83 (2011) 930–936.
[3] G. Lazarova, L. Genova, V. Kostov, Acta Biotechnol. 7 (1987) 97–99.
[4] H. Lidén, A.R. Vijayakumar, L. Gorton, G. Marko-Varga, J. Pharm. Biomed. Anal. 17 (1998) 1111–1128.
[5] A.K. Wanekaya, M. Uematsu, M. Breimer, O.A. Sadik, Sensors Actuators B: Chem. 110 (2005) 41–48.
[6] J.A. Ragazzo-Sanchez, P. Chalier, C. Ghommidh, Sensors Actuators B: Chem. 106 (2005) 253–257.
[7] W.H. Gao, Y.S. Chen, J. Xi, S.Y. Lin, Y.W. Chen, Y.J. Lin, Z.G. Chen, Biosens. Bioelectron. 41 (2013) 776–782.
[8] C.A. Lee, Y.C. Tsai, Sensors Actuators B: Chem. 138 (2009) 518–523.
[9] P. Yu, H. Zhou, H.J. Cheng, Q. Qian, L.Q. Mao, Anal. Chem. 83 (2011) 5715–5720.
[10] L. Wu, J.P. Lei, X.J. Zhang, H.X. Ju, Biosens. Bioelectron. 24 (2008) 644–649.
[11] M.M. Barsan, C.M.A. Brett, Talanta 74 (2008) 1505–1510.
[12] M. Zhou, Y.M. Zhai, S.J. Dong, Anal. Chem. 81 (2009) 5603–5613.
[13] V. Serafín, L. Agüí, P. Yáñez-Sedeño, J.M. Pingarrón, J. Electroanal. Chem. 656 (2011) 152–158.
[14] H. Teymourian, A. Salimi, R. Hallaj, Talanta 90 (2012) 91–98.
[15] M. Das, P. Goswami, Bioelectrochemistry 89 (2013) 19–25.
[16] A. Azevedo, D. Prazeres, J. Cabral, L. Fonseca, Biosens. Bioelectron. 21 (2005) 235–247.
[17] M.A. Hayes, W.G. Kuhr, Anal. Chem. 71 (1999) 1720–1727.
[18] S. Park, H. Boo, T.D. Chung, Anal. Chim. Acta 556 (2006) 46–57.
[19] A. Radoi, D. Compagnone, Bioelectrochemistry 76 (2009) 126–134.
[20] L. Zhang, Y. Li, L. Zhang, D.W. Li, D. Karpuzov, Y.T. Long, Int. J. Electrochem. Sci. 6 (2011) 819–829.
[21] C.S. Shan, H.F. Yang, D.X. Han, Q.X. Zhang, A. Ivaska, L. Niu, Biosens. Bioelectron. 25 (2010) 1504–1508.
[22] J.F. Ping, Y.X. Wang, K. Fan, J. Wu, Y.B. Ying, Biosens. Bioelectron. 28 (2011) 204–208.
[23] L.N. Wu, X.J. Zhang, H.X. Ju, Anal. Chem. 79 (2007) 453–458.
[24] L. Bai, D. Wen, J.Y. Yin, L. Deng, C.Z. Zhu, S.J. Dong, Talanta 91 (2012) 110–115.
[25] M.G. Zhang, C. Mullens, W. Gorski, Anal. Chem. 79 (2007) 2446–2450.
[26] H.Z. Li, H. Wen, S. Calabrese-Barton, Electroanalysis 24 (2012) 398–406.
[27] R.A. Mundaca, M. Moreno-Guzmán, M. Eguílaz, P. Yáñez-Sedeño, J.M. Pingarrón, Talanta 99 (2012) 697–702.
[28] A. Heller, B. Feldman, Chem. Rev. 108 (2008) 2482–2505.
[29] J. Wang, Chem. Rev. 108 (2008) 814–825.
[30] P.H. Ku, C.Y. Hsiao, M.J. Chen, T.H. Lin, Y.T. Li, S.C. Liu, K.T. Tang, D.J. Yao, C.M. Yang, Langmuir 28 (2012) 11639–11645.
[31] A. Walcarius, TrAC-Trends Anal. Chem. 38 (2012) 79–97.
[32] J.C. Ndamanisha, L.P. Guo, Anal. Chim. Acta 747 (2012) 19–28.
[33] R. Ryoo, S.H. Joo, M. Kruk, M. Jaroniec, Adv. Mater. 13 (2001) 677–681.
[34] C. He, X.J. Hu, Adsorption 18 (2012) 337–348.
[35] M. Kruk, Z.J. Li, M. Jaroniec, W.R. Betz, Langmuir 15 (1999) 1435–1441.
[36] J.F. Ping, Y.X. Wang, K. Fan, J. Wu, Y.B. Ying, Biosens. Bioelectron. 28 (2011) 204–209.
[37] X.Y. Jiang, L.D. Zhu, D.X. Yang, X.Y. Mao, Y.H. Wu, Electroanalysis 21 (2009) 1617–1623.
[38] F. Pariente, F. Tobalina, G. Moreno, L. Hernández, E. Lorenzo, H.D. Abruña, Anal. Chem. 69 (1997) 4065–4075.
[39] F. Moussy, S. Jakeway, D.J. Harrison, R.V. Rajotte, Anal. Chem. 66 (1994) 3882–3888.
[40] M.H. Huang, H.Q. Jiang, J.F. Zhai, B.F. Liu, S.J. Dong, Talanta 74 (2007) 132–139.
[41] H. Gülce, A. Gülce, M. Kavanoz, H. Coşkun, A. Yıldız, Biosens. Bioelectron. 26 (2002) 517–521.
[42] K. Guo, K. Qian, S. Zhang, J.L. Kong, C.Z. Yu, B.H. Liu, Talanta 85 (2011) 1174–1179.
[43] X.Q. Liu, B.H. Li, M. Ma, G.Q. Zhan, C.X. Liu, C.Y. Li, Microchim. Acta 176 (2012) 123–129.
[44] X.Q. Liu, B.H. Li, X. Wang, C.Y. Li, Microchim. Acta 171 (2010) 399–405.
[45] C.S. Shan, H.F. Yang, D.X. Han, Q.X. Zhang, A. Ivaska, L. Niu, Biosens. Bioelectron. 25 (2010) 1504–1508.
[46] D.W. Yang, H.H. Liu, Biosens. Bioelectron. 25 (2009) 733–738.
[47] S.N. Liu, C.X. Cai, J. Electroanal. Chem. 602 (2007) 103–114.
[48] Y.C. Tsai, J.D. Huang, C.C. Chiu, Biosens. Bioelectron. 22 (2007) 3051–3056.